Aquaculture Reports 23 (2022) 101077

Contents lists available at ScienceDirect

Aquaculture Reports

journal homepage: www.elsevier.com/locate/aqrep

Generation of ornamental Nile tilapia with distinct gray and black body color pattern by *csf1ra* mutation

Baoyue Lu [a], Chenxu Wang [a], Guangyuan Liang [a], Mengmeng Xu [a], Thomas D. Kocher [b], Lina Sun [a,*], Deshou Wang [a,*]

[a] *Key Laboratory of Freshwater Fish Reproduction and Development (Ministry of Education), Key Laboratory of Aquatic Science of Chongqing, School of Life Sciences, Southwest University, 400715 Chongqing, PR China*

[b] *The Department of Biology, University of Maryland, College Park, MD 20742, United States*

ARTICLE INFO

Keywords:
csf1ra mutation
CRISPR/Cas9
Color pattern
Nile tilapia

ABSTRACT

Nile tilapia (*Oreochromis niloticus*) is an important species in aquaculture and an excellent model fish for studying teleost color patterns. Colony-stimulating factor 1 receptor a (*csf1ra*) is critical for xanthophores development and body color formation in zebrafish and guppy. In this study, we established *csf1ra* mutant lines with two different targets by CRISPR/Cas9 in Nile tilapia. Unlike the wild type fish (WT) with vertical bars, the homozygous mutants showed two different color patterns, either uniformly gray (GT) or gray with black tail (BT). Compared with WT, the mutants had fewer melanophores, a few xanthophores and no erythrophores. Increased numbers of melanophores were observed in the tail of BT mutants. However, the establishment of early embryonic pigment cell precursors and the appearance of melanophores on the body were independent of *csf1ra*. In contrast, the appearance of xanthophores on the body and the formation of the vertical bar pattern dependent on the late metamorphic melanophores required *csf1ra*. The deletion of xanthophores and erythrophores caused by *csf1ra* mutation changed the body color pattern of Nile tilapia. These results demonstrated that *csf1ra* activity is essential for the development of erythrophores, late developing xanthophores and late metamorphic melanophores. These mutants provided good models for analyzing the genetic basis of tilapia body color pattern formation. Our study may help deepen the understanding of the formation of fish body color pattern, especially for cichlids with vertical bars. In addition, the mutants might be developed as ornamental fish (BT) or new strains for aquaculture.

1. Introduction

Unlike endothermic vertebrates that have a single neural crest-derived pigment cell type, the melanocyte, ectothermic vertebrates exhibit six classes of pigment cells, melanophores, xanthophores, erythrophores, iridophores, leucophores and cyanophores, collectively referred to as chromatophores (Fujii, 2000; Herbomel et al., 2001; Parichy, 2006; Kelsh et al., 2009; Mills and Patterson, 2009). The arrangement of these cells generates the pigment pattern in teleosts (Johnson et al., 1995; Hirata et al., 2003). The model fishes, medaka (*Oryzias latipes*) and zebrafish (*Danio rerio*), have melanophores, xanthophores and iridophores (Parichy and Turner, 2003a; Fang et al., 2018). The black melanophores contain melanin and are the ectotherm equivalent of melanocytes. The yellow or orange xanthophores contain carotenoids and pteridines. The iridescent iridophores contain purine rich reflecting platelets (Sköld et al., 2016).

Unlike medaka and zebrafish, cichlids have four pigment cell types, melanophores, xanthophores, iridophores and erythrophores, and display a variety of body colors and pigment patterns. Nile tilapia (*Oreochromis niloticus*), a cichlid species that is important in aquaculture (Chen et al., 2018; FAO, 2020), has emerged as a model system for studies of pigment pattern formation and chromatophore biology (Wang et al., 2021; Lu et al., 2022). Their body color and low contrast black bars make them unattractive to consumers in some countries (Hilsdorf et al., 2002; Zhu et al., 2016). Therefore, it is of great significance to improve tilapia body color patterns.

Abbreviations: dpf, days post fertilization; CRISPR/Cas9, clustered regularly interspaced short palindromic repeats/CRISPR associated protein 9; WT, wild type; GT, gray tail mutants; BT, black tail mutants.

* Corresponding authors.
E-mail addresses: sunlina@swu.edu.cn (L. Sun), wdeshou@swu.edu.cn (D. Wang).

https://doi.org/10.1016/j.aqrep.2022.101077
Received 14 January 2022; Received in revised form 26 February 2022; Accepted 2 March 2022
Available online 4 March 2022
2352-5134/© 2022 The Authors. Published by Elsevier B.V. This is an open access article under the CC BY-NC-ND license (http://creativecommons.org/licenses/by-nc-nd/4.0/).

Xanthophores play an important role in the formation of body color pattern in zebrafish and guppy, *Poecilia reticulata* (Parichy and Turner, 2003b; Kottler et al., 2013), but little is known about the role of erythrophores in fish body color pattern formation. Both erythrophores and xanthophores store carotenoids. In addition, erythrophores function to produce signals in a variety of fitness-relevant contexts including mate choice, social competition and species recognition in cichlids (Ahi et al., 2020).

The body of adult Nile tilapia is composed of 7–9 black vertical bars separated by light interbars (Wang et al., 2021; Lu et al., 2022). The vertical bar pattern of Nile tilapia is different from the horizontal stripe pattern of zebrafish. The black stripes of zebrafish are mainly composed of melanophores, and the bright interstripes are mainly composed of xanthophores. There is an obvious boundary between black stripes and interstripes, as well as between melanophores and xanthophores (Parichy and Turner, 2003a). Several lines of evidence indicate the stripes form in part due to interactions between melanophores and xanthophores (Parichy et al., 2000a; Maderspacher and Nüsslein-Volhard, 2003). In addition, by comparing the composition and development of stripes, bars and spots in two cichlid species, it is shown that stripes develop by differentiation of melanophores along horizontal myosepta, while bars do not develop along obvious anatomical boundaries and increase in number in relation with body size. Therefore, it is proposed that metamorphic melanophore differentiation and migratory arrest upon arrival to the skin lead to stripe formation, while bar formation must be supported by extensive migration of undifferentiated melanophores in the skin (Hendrick et al., 2019). However, it is unclear whether the formation of a vertical bar pattern in Nile tilapia involves the same mechanism. In addition, it is unclear whether xanthophores and erythrophores also play important roles in the formation of vertical bars.

The number of genes which are known to affect carotenoid- and pteridine-based pigment cells in vertebrates is rather small, especially those related to erythrophores. In zebrafish, *csf1ra*, a tyrosine kinase receptor and a key regulator of macrophage lineage cells, has also been found to be expressed in neural crest progenitors and plays an important role in xanthophore development and color pattern formation (Parichy et al., 2000a; Parichy and Turner, 2003a; Salzburger et al., 2007; Tripathy et al., 2019). C*sf1ra* is essential for xanthophore development in guppy, as mutation of *csf1ra* is responsible for the *blue* mutant, in which the skin lacks orange pigmentation (Kottler et al., 2013). Comparative studies suggest some functional diversification of *csf1ra* even within the same genus (Parichy, 2006; Kottler et al., 2013). However, the function of *csf1ra* is less well understood in other teleost species, especially in cichlids, which are rich in erythrophores and xanthophores and shows gorgeous and diverse body colors. Moreover, little is known about the genes affecting erythrophore development, because there are no erythrophores in model organisms such as zebrafish and medaka.

Studies in zebrafish showed that there are two different types of melanophores, early- and late-appearing metamorphic melanophores, which are regulated by two tyrosine kinase receptor genes, *kit* and colony-stimulating factor 1 receptor a, *csf1ra*, respectively (Parichy et al., 1999, 2000a, 2000b; Parichy and Turner, 2003b; Lang et al., 2009). These two types of melanophores play key roles during the establishment of the adult zebrafish pigment pattern (Parichy et al., 1999, 2000a, 2000b; Parichy and Turner, 2003b). Studies in guppy have also shown that two temporally and genetically distinct melanophore populations contribute to the adult pattern formation: one early appearing and *kit*-dependent and the other late-developing and *kit*-independent (Kottler et al., 2013). However, it is unclear whether these same two types of melanophores exist in other teleosts, and whether the late-appearing melanophores are dependent on *csf1ra*.

In this study, we generated *csf1ra* homozygous mutant lines with two different target sites using the CRISPR/Cas9 technology and obtained two different body color patterns, gray tail (GT) and black tail (BT) from one target site, and only GT from the other target site in Nile tilapia. We analyzed the phenotype of GT and BT mutants and demonstrated that *csf1ra* is crucial for the late-appearing melanophores, vertical bar formation and development of xanthophores and erythrophores.

2. Materials and methods

2.1. Animals

The Nile tilapia in our laboratory was first introduced from Japan (Prof. Nagahama's lab, National Institute for Basic Biology), expanded by multi-generation propagation and established a stable strain. Fish were raised in recirculating aerated freshwater tanks at 26 °C under a natural photoperiod. Fertilized eggs were obtained by artificial fertilization and incubated in an artificial incubation system in re-circulating water at 26 °C to obtain fry. Animal experiments were conducted in accordance with the regulations of the Guide for Care and Use of Laboratory Animals and were approved by the Committee of Laboratory Animal Experimentation at Southwest University.

2.2. Establishment of csf1ra mutant line in Nile tilapia

Two target sites in the 3rd (target 1) and 2nd (target 2) exon of *csf1ra* were selected to establish the homozygous mutant line. The *csf1ra* chimera (F0) of each target was generated by CRISPR/Cas9, as described previously in Nile tilapia (Wang et al., 2021). Briefly, gRNA and Cas9 mRNA were co-injected into one-cell stage embryos at a concentration of 150 ng/μl and 500 ng/μl, respectively. Twenty embryos were collected 72 h after injection. Genomic DNA was extracted from pooled control and injected embryos and used for the mutation assays. DNA fragments (365 bp) spanning the target 1 were amplified using the primers *csf1ra*-F1 GGTGGTAGTGAAGGAGGGTGAG and *csf1ra*-R1 CAGAGACAGAAGCAGCCAGTGA. DNA fragments (378 bp) spanning the target 2 were amplified using the primers *csf1ra*-F2 TGGAGCCAAGAGTCTTCAATCT and *csf1ra*-R2 TGTAGCGTCTGTGTTTGGGTAG. The mutated sequences were analyzed by restriction enzyme digestion and Sanger sequencing. The *csf1ra* heterozygous XX, XY offspring were obtained by mating a chimeric XY male with wild type (WT) XX females and mutated sequences were confirmed by Sanger sequencing. The siblings of heterozygous mutants carrying the same mutation were mated to generate homozygous mutants. Each PCR mixture contained 15 μl 2 × Taq MasterMix (Vazyme Biotech, Nanjing, China), 0.5 μl each specific primer (10 μM), 1 μl DNA (100 ng), and 13 μl double distilled water (DDW), for a total volume of 30 μl. The PCR cycling conditions were: one cycle at 95 °C for 3 min; 32 cycles at 95 °C for 30 s, 60 °C for 30 s, and 72 °C for 30 s for both target sites; one cycle of 72 °C for 10 min. In addition, the desired band (the uncleaved band) was extracted from a 1.8% agarose gel using a Gel Extraction Kit (BIOER technology, Hangzhou, China) and sub-cloned into pMD19-T vector (Takara, Dalian, China), according to the manufacturer's instructions. The positive clones were isolated with M13 forward and reverse primers synthesized by BGI (Beijing, China) and then sent to BGI (Beijing, China) for sequencing. The resulting sequences were precisely aligned using Lasergene software suite (DNAStar, Inc. Madison, WI, USA).

2.3. DNA extraction

Genomic DNA samples were obtained from embryos or tail fin clips. DNA was isolated by phenol/chloroform extraction following proteinase (Sigma, Germany) digestion, as previously described (Sambrook et al., 1989). After two phenol-chloroform, and one chloroform extraction, DNA was precipitated with one volume of isopropanol. DNA was collected by centrifugation at 4 ℃, washed with 70% ethanol, then washed with absolute ethanol, dried, and dissolved in DDW. The quality and concentration of DNA were then assessed by agarose gel electrophoresis, and measured using a NanoDrop 2000 spectrophotometer (Thermo Fisher Scientific, Wilmington, DE, USA). Finally, the DNA was diluted to a concentration of 100 ng/μl, and stored at − 20 °C for future

use.

2.4. Genetic analysis of GT and BT

GT and BT mutants were raised to 240 days post fertilization (dpf) for mating experiment. Three females and one male were put into an independent breeding pool (1.5 m × 2 m) and fed three times a day. There were four groups: BT female × GT male, GT female x BT male, BT female x BT male and GT female × GT male, with three repetitions in each group. The fry were removed from the breeding pool every 14 days, and each batch of fry was raised separately. At 90 dpf, the numbers of GT or BT phenotype in each batch of offspring was recorded.

2.5. Phenotype analysis and image capture

GT and BT individuals used for phenotype analysis were derived from the offspring of GT x GT mating and BT × BT mating, respectively, since these two crosses produced all GT and BT offspring. Fish at 4, 6, 10, 40, 90, 240 dpf were sampled for phenotype analysis. Wild type fish as the same stages were used as control. For imaging of live specimens, individuals with the same development period and similar body shape were selected and anesthetized with Tricaine (Sigma-Aldrich, Shanghai, China) at a concentration of 4.5 mg/mL. Then, L-Adrenaline treatment (Sigma-Aldrich, Shanghai, China) was carried out at a concentration of 4.5 mg/mL to shrink the pigment cells. (Hendrick et al., 2019). To calculate the number of melanophores and xanthophores, Leica M165FC stereomicroscope was used to image WT, GT, BT at 4, 6, 10, 40 dpf. The skin and tail fin of 90 dpf and adult fish (240 dpf) were also imaged by this stereomicroscope. Three months old fish and adult fish images were taken with a Canon SLR camera 700D (Canon, Taiwan). The number of melanophores in the unilateral body surface (including the yolk sac) was calculated using 6 fish for each strain at 4 dpf and 6 dpf. The number of melanophores and xanthophores in the skin and tail fin were calculated using 6 fish for each strain at 40 dpf, 90 dpf and 240 dpf. Chromatophore density averages were obtained from regions representative of each pattern in WT, GT or BT (n = 6). Image processing was performed in Adobe Photoshop (CC2019).

2.6. Statistical analysis

Data are expressed as mean ± SD. Significant differences in the data among groups were tested either by two-way ANOVA followed by Sidak's multiple comparisons test or by one-way ANOVA followed by Tukey test. $P < 0.05$ was considered to be statistically significant. All

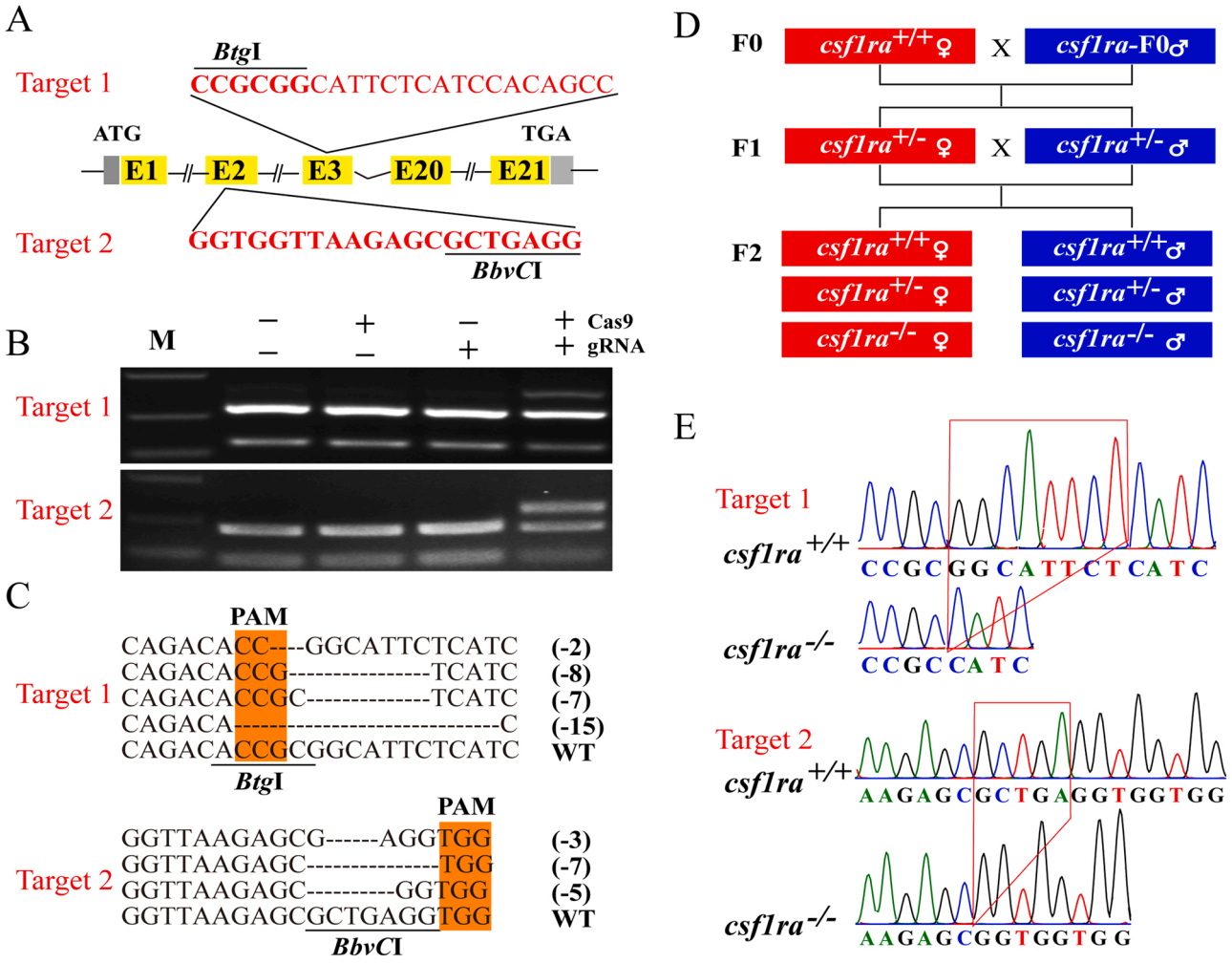

Fig. 1. Establishment of *csf1ra* mutant lines by CRISPR/Cas9 in Nile tilapia. Gene structures of *csf1ra* showing two target sites and restriction site of *Btg*I in target 1 and *Bbv*CI in target 2 (A). The indels in F0 mutants were confirmed by two assays, restriction enzyme digestion (B) and Sanger sequencing (C). The Cas9 mRNA and gRNA were added as indicated. Sanger sequencing results from the uncleaved band were listed. Deletions are marked by dashes, and the PAM is marked in light orange. The number (-) on the right side of the sequence indicates the bases loss of each allele. Schematic diagram showing the breeding plans of two targets from F0 to F2 fish (D). Successful establishment of the homozygous mutant lines (− 8 bp) of target 1 and (− 5 bp) of target 2 was confirmed by Sanger sequencing (E). M, DNA Marker DL2000.

analyzes were performed using GraphPad Prism Version 8.0.1 (GraphPad Software Inc, San Diego, CA, USA).

3. Results

3.1. Generation of csf1ra mutants by CRISPR/Cas9

The CRISPR/Cas9 gene editing method was used to create *csf1ra* homozygous mutants in Nile tilapia as reported previously by our group (Wang et al., 2021; Lu et al., 2022). We designed a target (target 1) on the third exon of *csf1ra* and established a homozygous mutant line. However, when homozygotes grew to 90 dpf, we observed two different body color pattern phenotypes, either uniformly gray (GT) or gray body with black tail (BT), although they had the same base deletion at the target site 1. In order to be sure these phenotypes of GT and BT were produced due to *csf1ra* mutation, we designed a second target (target 2) on the second exon of *csf1ra* and established the homozygous mutant line. However, only GT phenotype was observed in the homozygous mutants of target 2. The breeding plan for establishment of mutant lines homozygous for each target is shown in Fig. 1. Sequences containing *Btg*I restriction site (target 1) and *Bbv*CI restriction site (target 2) adjacent to proto-spacer adjacent motif (PAM) of *csf1ra* gene of Nile tilapia were selected as target sites (Fig. 1A). The guide RNA and CRISPR/Cas9 RNA were injected into one cell stage embryos obtained by crossing male and female. Genomic DNA from 20 pooled injected embryos of target 1 and target 2 were extracted and used as template for PCR amplification and mutation assays, respectively. The amplified products of target 1 and target 2 were completely digested by restriction enzyme to produce 232 bp, 133 bp and 280 bp, 98 bp fragments, respectively, while intact DNA fragments of approximately 365 bp of target 1 and approximately 378 bp of target 2 were observed in embryos injected with both Cas9 mRNA and target guide RNA (Fig. 1B). Representative Sanger sequencing results from the uncleaved bands are listed, which confirmed in-frame-shift or frame-shift deletions induced at the target sites (Fig. 1C). The XX, XY *csf1ra* heterozygous mutants (F1) were obtained by mating the chimera male with WT female. The allele of 8 bp deletion of target 1 and the allele of 5 bp deletion of target 2 in F1 offspring were selected to breed the F2 generation (Fig. 1D). Due to the obvious body color difference, the *csf1ra*$^{-/-}$ individuals were easily distinguished in F2 population, and then confirmed by Sanger sequencing (Fig. 1E).

3.2. Melanophores significantly reduced in csf1ra homozygous mutants during larval stages

In order to understand how the pigment pattern develops in *csf1ra* homozygous mutants, images of wild type (WT), black tail (BT) and gray tail (GT) individuals were taken during larval stages. Melanophores were the first chromatophores to appear, on the yolk sac at about 27–30 h post fertilization (Fujimura and Okada, 2007; Wang et al., 2021). In the present study, we also observed the appearance of melanophores in WT, BT and GT at the same stage. Compared with WT, both GT and BT showed no significant difference in melanophore numbers on the body at 4 dpf, but they had significantly fewer melanophores at 6 dpf (Fig. 2A–F; Fig. 3). The difference increased further and could be distinguished by the naked eye at 10 dpf (Fig. 2G–L). This difference was because the increase in the number of melanophores in GT and BT was lower than that in WT, rather than a higher rate of melanophore apoptosis in GT and BT, since the total number of melanophores in WT, GT and BT all increased significantly from 4 to 6 dpf (Fig. 3). At 6 dpf and 10 dpf, we detected the appearance of light colored xanthophores, both on the head and trunk of WT individuals (Fig. 2D, G), but only on the head of both GT (Fig. 2E, H) and BT (Fig. 2F, I) mutants.

3.3. No bars, no erythrophores and only a few xanthophores in csf1ra mutants at 40 and 90 dpf

Melanophores, xanthophores and iridophores were observed in both bars and interbars in WT at 40 dpf, indicating that they were composed of the same pigment cell types (Fig. 4A, D). Significant differences were observed for melanophore density, with densities higher in the bars than in the interbars, while no such differences were observed for xanthophore density (Fig. 4A, D, R). In addition, significant differences were

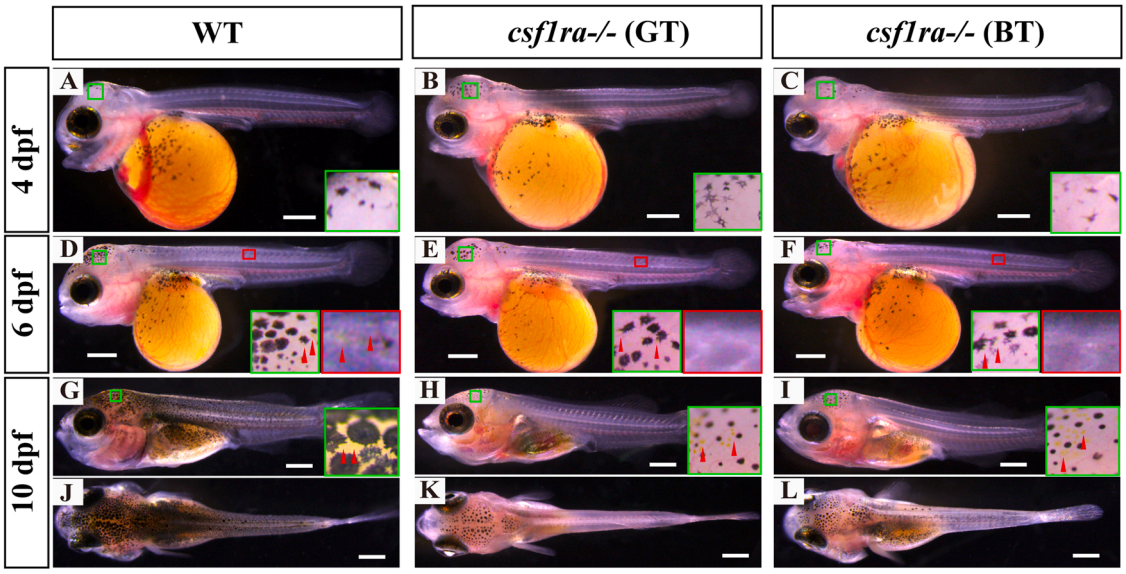

Fig. 2. Comparative analysis of melanophores and xanthophores in the body surface (including the yolk sac) of WT and *csf1ra* mutants from 4 to 10 dpf. Melanophore and xanthophore numbers increased with the development of WT and *csf1ra* homozygous mutants from 4 to 10 dpf. At 4 dpf, there were no xanthophores and no differences in morphology or number of melanophores were observed in WT (A), GT (B) and BT (C). At 6 dpf, the light colored xanthophores appeared both on the head (green box of D) and trunk (red box of D) of WT individuals (D), while only a few xanthophores appeared on the head in both *csf1ra* mutants GT (E) and BT (F). At 10 dpf, more xanthophores appeared on the head of WT (G), GT (H) and BT (I). The number of melanophores in GT (H, K) and BT (I, L) are significantly less than that in WT (G, J). Pictures in the lower right are higher magnifications of the green box and red box area. Red arrow heads indicate xanthophores. dpf, days post fertilization; WT, wild type fish; GT, gray tail phenotype appears after 90 dpf; BT, black tail phenotype appears after 90 dpf; scale bar in A–L, 1 mm.

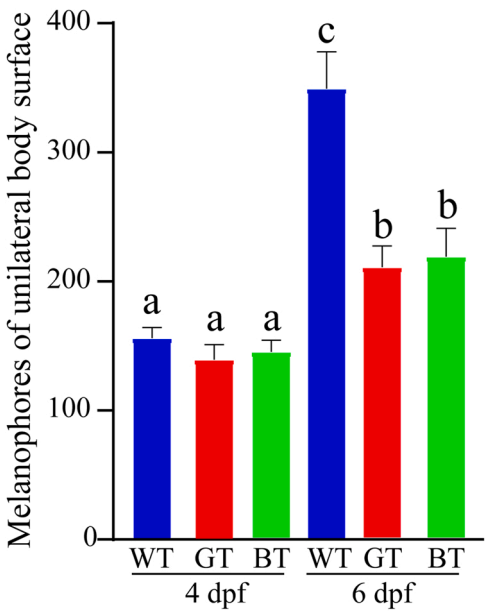

Fig. 3. Statistical analysis of melanophore number in unilateral body surface (including yolk sac) of WT and *csf1ra* mutants at 4 and 6 dpf. The melanophores increased significantly with development in WT, GT and BT. There were no significant differences in melanophore numbers in WT, GT and BT at 4 dpf, and significant increasing of melanophores were observed at 6 dpf in WT, GT and BT. Significantly higher melanophore numbers were observed in WT than those in GT and BT which displayed no significant difference between themselves. Data are presented as mean ± SD (n = 6 each). Different letters above the error bar indicate significant differences at $p < 0.05$, as determined by two-way ANOVA followed by Sidak's multiple comparisons test. dpf, days post fertilization; WT, wild type fish; GT, gray tail phenotype appears after 90 dpf; BT, black tail phenotype appears after 90 dpf.

also observed in the density of melanophores and xanthophores between dorsal and ventral areas bounded by the horizontal myosepta (Fig. 4A, D, Q), with densities in the dorsal areas higher than the ventral (Fig. 4A, D, F, I, K, N). Unlike the WT (Fig. 4A, D; Fig. S1), no pattern of bars and interbars was observed for BT and GT mutants. A few xanthophores were restricted to the top of the head, and almost no xanthophores were observed on the trunk and tail fin (Fig. 4F, I, K, N; Fig. S1). Melanophore numbers were significantly reduced in BT and GT mutants compared with WT (Fig. 4C, E, H, J, M, O, P, S; Fig. S1). The melanophores were evenly distributed in BT and GT mutants (Fig. 4I, N, R). The highest density of melanophores was observed in the dorsal bar, followed by the ventral bar, the dorsal interbar in WT, the dorsal skin of GT and BT, and then the ventral interbar in WT, the ventral skin of GT and BT (Fig. 4D, I, N, R). No erythrophores were observed in WT, BT and GT at 40 dpf (Fig. 4). The erythrophores appeared on the head, ventral skin, dorsal fin, anal fin and tail fin in WT around 50 dpf and were maintained into adult stages (Wang et al., 2021).

The phenotypic differences between BT and GT appeared at around 90 dpf (Fig. 5A–C). Different from the body color pattern of WT with bars and interbars (Fig. 5A), the body color of GT was uniform gray (Fig. 5B). Most of the trunk of BT was the same gray as GT, but the tail (including the peduncle, posterior dorsal fin, anal fin and tail fin) became light black with increased melanophores at 90 dpf (Fig. 5C, D). In WT, there were almost no erythrophores in bar and interbar of trunk surface but many erythrophores were observed on the ventral skin and tail fin, while no erythrophores were observed on the ventral skin and tail fin in GT and BT (Fig. 5A–C).

3.4. Adult pigment pattern of WT, BT and GT

At least four types chromatophores (melanophores, xanthophores, iridophores and erythrophores) were observed in adult WT (Fig. 6A, D), as described previously (Wang et al., 2021; Lu et al., 2022). The body of WT is composed of 7–9 dark vertical bars and light interbars (Fig. 6A). Similarly, dark or light bars were also formed on the tail fin of WT (Fig. 6A, D). However, no bars or interbars were observed on the body trunk or tail fin in GT and BT mutants (Fig. 6B, C). The whole trunk and all fins of GT are uniformly gray, so the phenotype is defined as gray tail "GT" (Fig. 6B). The trunk anterior to the caudal peduncle, pectoral fin, ventral fin, most dorsal fin and part of anal fin of BT (Fig. 6C) displayed the same uniform gray color as GT (Fig. 6B), while the dorsal fin end, anal fin, entire caudal peduncle and tail fin became dark black (Fig. 6C), and therefore, the phenotype is defined as black tail "BT". More xanthophores and erythrophores were observed in the bars than in the interbars of tail fins in WT (Fig. 6D), but not in GT (Fig. 6E) and BT (Fig. 6F) which displayed an absence of both types of pigment cells. The highest density of melanophores was observed on the caudal peduncle in BT (Fig. 6C), followed by bar in WT (Fig. 6A), and then interbar in WT (Fig. 6A), caudal peduncle in WT (Fig. 6A), pseudo bar (PB) in GT (Fig. 6B), caudal peduncle in GT (Fig. 6B), pseudo bar in BT (Fig. 6C), and there was no significant difference among the latter five (Fig. 6A–C, G). In addition, the density of melanophores on BT tail fin (Fig. 6F) was significantly higher than that on the bars of the tail fin in WT (Fig. 6D), and the tail fin of GT (Fig. 6E) was significantly higher than on the interbar of tail fin in WT (Fig. 6D, H).

3.5. Crosses and offspring statistics in different GT and BT combinations

To determine which phenotype is dominant, crosses were performed using GT and BT male and female fish in different combinations and repeated three times. The phenotype identification of GT and BT for the offspring was performed at 90 dpf for statistics (Fig. 7). Crosses of BT female and GT male produced BT:GT = 4:184 (1:45, 1:68, 2:71) (Fig. 7A). Crosses of GT female and BT male produced BT:GT = 2:254 (1:95, 0:82, 1:77) (Fig. 7B). Crosses of BT female with BT male produced BT:GT = 171:3 (64:1, 49:1; 58:1) (Fig. 7C). Crosses of GT female and GT male produced BT:GT = 0:179 (89, 54, 36) (Fig. 7D). Taken together, these results indicated that probably GT is dominant to BT. However, another generation (F2) is needed to determine whether it is controlled by one locus with a simple Mendelian inheritance.

4. Discussion

For more than a century, a large number of studies on pigment pattern mutants have identified many loci required for pigment cell development and pattern formation (Bennett and Lamoreux, 2003). Many mutants have obvious phenotypes limited to the pigment cells themselves, often reflecting defects in pigment synthesis and pigment cell development. However, some mutants exhibit pleiotropic defects in other neural crest derivatives or other organ systems (Zsebo et al., 1990; Besmer et al., 1993; Parichy et al., 2000a, 2000b; Parichy and Turner, 2003a, 2003b; Lang et al., 2009). In this study, we demonstrated that *csf1ra* plays an important role in the development of xanthophores, erythrophores and melanophores and is essential for the formation of body color pattern in Nile tilapia.

4.1. Melanophores with different temporal and spatial distribution were observed in Nile tilapia

As mentioned above, there are two types of melanophores in zebrafish. The early metamorphic melanophores require *kit* for their development, while the late metamorphic melanophores depend on *csf1ra*. Both play key roles during the establishment of the adult zebrafish pigment pattern (Parichy et al., 1999, 2000a, 2000b; Parichy and Turner, 2003b). Different from zebrafish, based on the observations of wild type fish and mutants, we speculate that Nile tilapia may have three types of melanophores regulated by different signals, and they

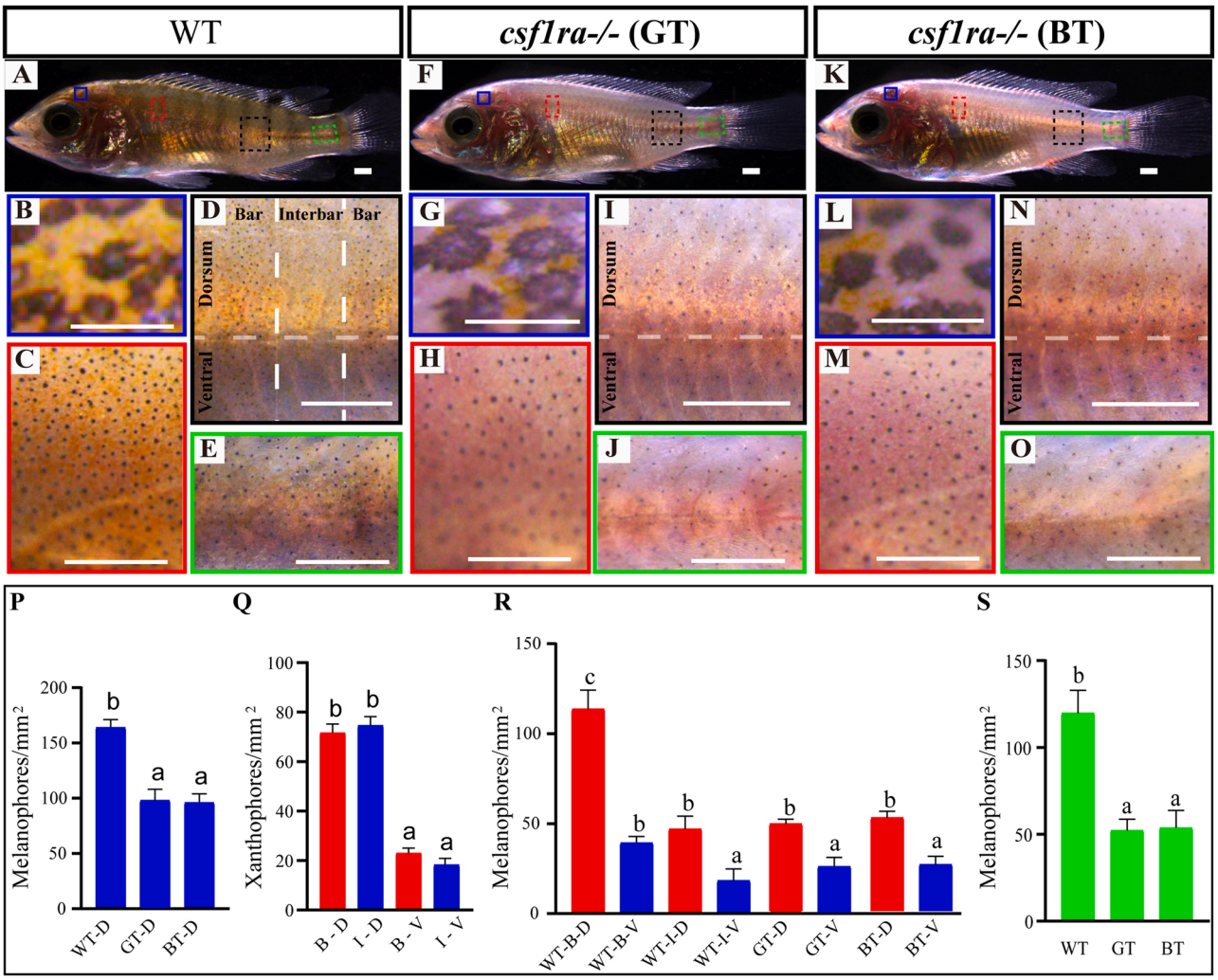

Fig. 4. Phenotype/color pattern of WT, GT and BT at 40 dpf. The WT, with obvious vertical bars, looked obviously darker than the mutant fish, while the mutant fish had no bars, and there was no significant difference in body color between GT and BT mutants (A, F, K). Both bars and interbars were composed of melanophores, xanthophores and iridophores in WT at 40 dpf (A, D), and more melanophores and xanthophores were observed in the dorsal skin than the ventral skin (D). More melanophores were observed in bars than interbars (D). At high magnification, there were obvious xanthophores in the head of both WT and mutants, but the WT had significantly more xanthophores than the mutants, and the yellow color was deeper (B, G, L). There were also a large number of xanthophores in the body of the WT (C, D), but there were almost no xanthophores in the body skin of mutants (H, I, M, N). The melanophores and xanthophores in the back of WT were obviously more than those in the abdomen, and the melanophores in the bars were obviously more than those in the interbars (D). The melanophores in the back of mutants were also significantly more than those in the abdomen (I, N). Consistently, the statistical analysis of C, H and M regions showed that the number of melanophores of the WT were significantly higher than those of the mutants (P). The statistical analysis of D, I and N regions showed that the number of melanophores in the bars was significantly higher than that in the interbars. There was no significant difference in xanthophore numbers, both at the dorsal and ventral side, between the bars and the interbars (Q), and the number of melanophores and xanthophores at the dorsal side was significantly higher than those at the ventral side (R). The number of melanophores in the mutants was significantly lower than that in the WT, and the number of melanophores in the dorsal side was also higher than that at the ventral side (R). Similarly, the statistics of E, J and O regions showed that the number of melanophores in the peduncle of WT was also significantly higher than that of mutants (S). The picture framed with different colored lines under each fish (B–E, G–J, L–O) corresponds to the area surrounded by small boxes of the same color in A, F and K, respectively. P shows the melanophore density of C, H and M. Q shows the xanthophore density of D. R shows the melanophore density of D, I and N. S shows the melanophore density of E, J and O. Data are presented as mean ± SD (n = 6 each). Different letters above the error bar indicate significant differences at $p < 0.05$, as determined by one-way ANOVA followed by Tukey test. dpf, days post fertilization; WT, wild type fish; GT, gray tail phenotype appears after 90 dpf; BT, black tail phenotype appears after 90 dpf; D, dorsum; V, ventral; B, bar; I, interbar; scale bar in A–O, 1 mm.

have different temporal and spatial distribution: One type of melanophores was appeared from embryo to early larval stage (6 dpf), which is independent of *csf1ra* signal. The second type of melanophores developed from late larval stage and depended on the *csf1ra* signal, is crucial for the formation of bar pattern in tilapia. The third type of melanophores was appeared on the tail of BT after 90 dpf, but the gene responsible for this phenotype is still unclear. Of course, more evidences of different cellular function or structure are needed to prove whether they are different type or sub-type of melanophores. Our data demonstrated that the melanophores on the tail of BT were newly differentiated, and not migrating in from the gray area, as no differences in melanophore density were observed in gray area between the GT and BT. The first two types of melanophores are crucial for the formation of body color patterns in late larval stage, juvenile stage and adult stage of Nile tilapia. However, the switch of the emergence of the third melanophore in BT remains unclear.

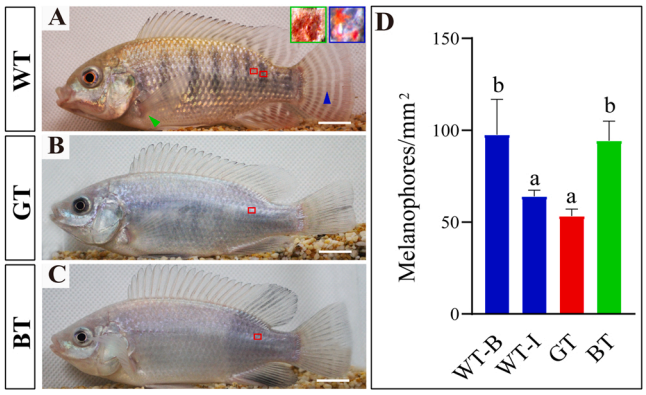

Fig. 5. Formation of body color pattern in WT, GT and BT at 90 dpf. Different from the body color pattern of WT (A), with bars and interbars, the body color of GT (B) and BT is uniformly gray, excepted that the peduncle and tail of the BT is black (C) due to increased melanophores at 90 dpf. A large number of erythrophores were observed on the ventral skin and tail fin of WT (green box and red box in A), while no erythrophores were observed in skin and tail fin of GT and BT. D shows statistical analysis of the melanophore density of red box in A–C. Data are presented as mean ± SD (n = 6 each). Different letters above the error bar indicate significant differences at $p < 0.05$, as determined by one-way ANOVA followed by Tukey test. dpf, days post fertilization; WT, wild type fish; GT, gray tail mutants; BT, black tail mutants; scale bar in A–C, 1 cm.

4.2. *There may be two types of xanthophores regulated by different signals in Nile tilapia*

The *csf1ra* promotes the migration of the xanthophore precursors from the neural crest and is essential for development of early larval and adult xanthophores in zebrafish (Parichy et al., 2000b). In *csf1ra* mutant zebrafish, all xanthophores fail to develop (Parichy and Turner, 2003a, 2003b). However, in Nile tilapia, even in the homozygous mutants of *csf1ra*, some xanthophores still appeared on the head at about 6 dpf. The number and time of appearance of these xanthophores was not significantly different between the mutants and WT. Compared with WT, few xanthophores were observed on the trunk or fins in mutants, because the development of these xanthophores requires *csf1ra* activity (a very small number of xanthophores independent of *csf1ra* activity occasionally appeared in some mutants). These findings suggest that there may be two types of xanthophores in Nile tilapia. One starts to develop on the head in the early stage of larvae, persists into the adult stage, and is independent of *csf1ra* signal. The other develops in the late larval stage, participates in the formation of the bar pattern, and requires *csf1ra* activity. Therefore, *csf1ra* is required for recruitment of pigment cell precursors to the fate of xanthophore from the late larval stage to the adult stage, but is not required for establishing a population of precursor cells during embryogenesis and early larval stage in Nile tilapia.

4.3. *The development of xanthophores and erythrophores were csf1ra dependent in Nile tilapia*

Cells characterized by high concentrations of carotenoids and pteridines are known as xanthophores or erythrophores (Ban et al., 2005; Chen et al., 2014, 2015). Several genes are known to affect carotenoid- and pteridine-based color diversity and development of xanthophores and erythrophores. For example, *BCO2* encodes a carotenoid-cleavage enzyme which is associated with yellow or white skin and plumage color polymorphism in domestic chicken (Eriksson et al., 2008), wood warblers (Toews et al., 2016) and an East African cichlid fish, *Tropheus duboisi* (Ahi et al., 2020); *CYP2J19* encodes a ketolase that catalyzes the metabolic conversion of dietary yellow carotenoids into red ketocarotenoids in birds and turtles (Twyman et al., 2016; Mundy et al., 2016; Lopes et al., 2016; Ahi et al., 2020); *SCARB1* encodes a high-density lipoprotein receptor that mediates the cellular uptake of carotenoids and was found to be responsible for the presence/absence of carotenoid plumage coloration in canary breeds (Toomey et al., 2017) and the body color of Oujiang color common carp, *Cyprinus carpio var. color* (Du et al., 2021). As described above, *csf1ra* was found to play an important role in the development and maintenance of xanthophores in zebrafish and guppy (Parichy and Turner, 2003b; Kottler et al., 2013). Tilapia have both xanthophores and erythrophores, while zebrafish and medaka have no erythrophores. Consistent with zebrafish and guppy, in this study, we demonstrated that *csf1ra* was necessary for the development of late metamorphic xanthophores. In addition, we demonstrated for the first time that *csf1ra* plays a key role in the development of erythrophores in Nile tilapia. In WT, erythrophores were mainly distributed in the head, ventral skin, anal fin and tail fin, but not in the vertical bar and interbar on the trunk surface. The number of erythrophores on the bar was more than that on interbar on tail fin. However, in *csf1ra* mutants, no erythrophores, xanthophores, bars and interbars were observed on the tail fin. Therefore, we speculate that erythrophores play an important role in the formation of the bar and interbar in the tail fin, but not the bar and interbar pattern on the trunk.

4.4. *The formation of vertical bars required the late metamorphic melanophores dependent on csf1ra signal*

The results of this study showed that *csf1ra* is not necessary to establish precursor cell populations during embryogenesis but is required for recruiting pigment cell precursors to a xanthophore and melanophore fate, with concomitant effects on chromatophore organization and formation of the bar pattern in Nile tilapia. These results are similar to those in zebrafish (Parichy and Turner, 2003a, 2003b). The black bars and light interbars of tilapia are both mainly composed of melanophores and xanthophores. Further, no significant differences in composition of pigment cell types and density of xanthophores (*csf1ra*-dependent) were observed between bar and interbar in wild-type individuals, and there was no obvious boundary between melanophores and xanthophores. Therefore, the distribution and density of xanthophores were probably not the cause of the formation of the bar and interbar. Rather, the existence of *csf1ra* dependent xanthophores and late-appearing metamorphic melanophores was essential for adult vertical bar pattern formation in Nile tilapia. But there was no direct evidence showing that melanophores interact with *csf1ra*-dependent xanthophores to form the adult bar pattern in Nile tilapia.

4.5. *The BT phenotype probably resulted from cryptic polymorphism at another locus*

In order to determine whether both GT and BT phenotypes were produced by *csf1ra* mutation, we designed a new target (target 2) on the second exon of *csf1ra* and established a homozygous mutant line. However, only GT was observed in the homozygous mutants of target 2. This showed that GT was indeed caused by the functional defect of *csf1ra* gene, while BT probably not. The mating experiment showed that the offspring from GT female and BT male and BT female and GT male were almost all GT, the offspring from GT female and GT male were all GT, while the offspring from BT female and BT male were almost all BT. A very small amount of BT appeared in the offspring from GT and BT, and a very small amount of GT from BT and BT, which may be caused by manual identification error or escape during breeding as some BT displayed none typical features. On this premise, GT is dominant for BT, since all the offspring of GT mating with BT were GT. As only 20% (3/15) of the homozygous mutants (F2) obtained by sibling cross of F1 heterozygous mutants displayed BT phenotype, we speculated that this may be caused by either off-target effect or cryptic variation. By blasting the sequence of target 1 against the genome sequence of Nile tilapia, we found potential off-target sequences (POTS) highly similar to the target 1 sequences. Primer pairs spanning the POTS were designed to amplify

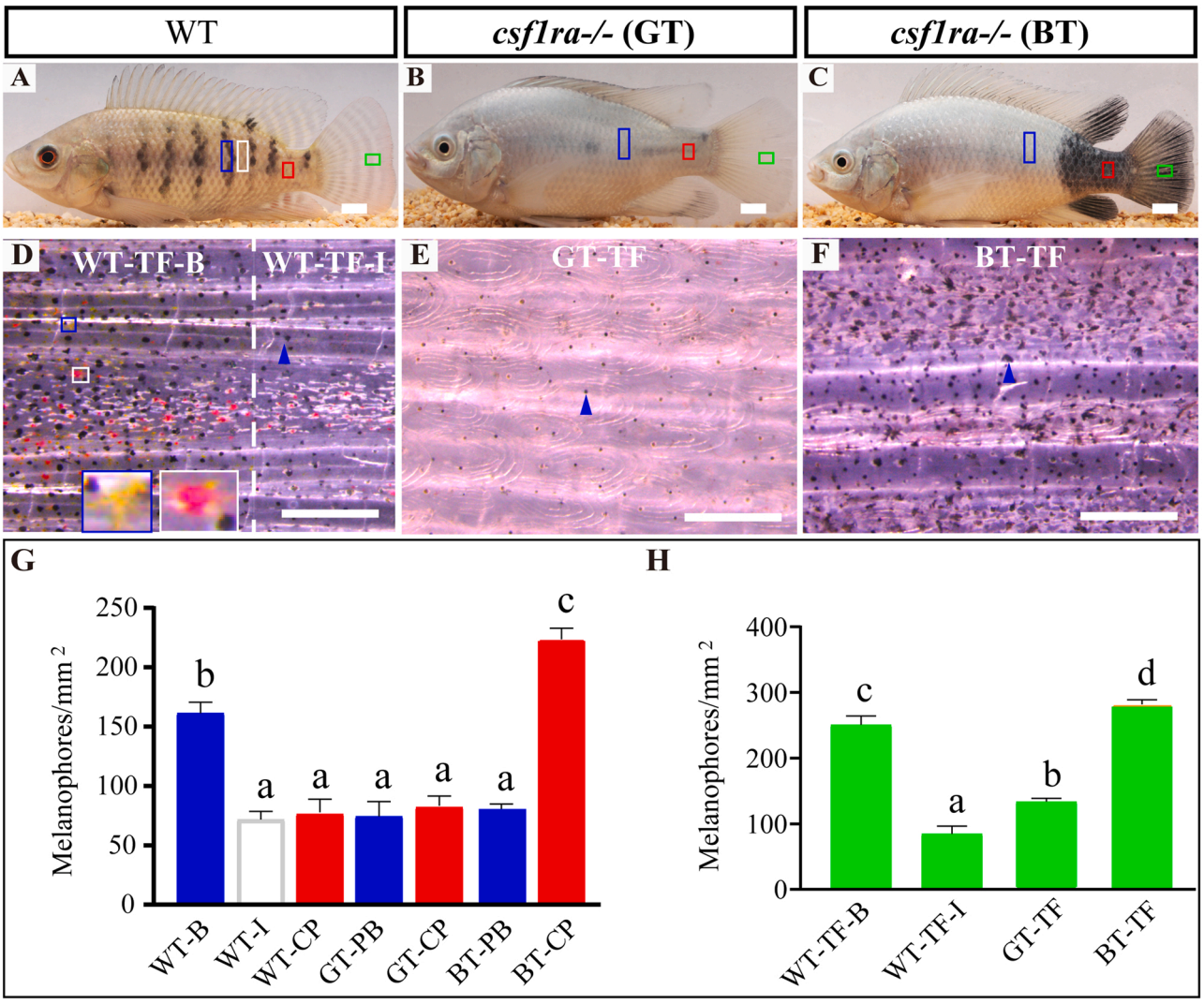

Fig. 6. Adult body color pattern of WT, GT and BT. (A–C) Body color of adult WT, GT and BT. Vertical bars were observed obviously on the trunk and tail fin of WT (A), while almost uniform gray body color pattern, with no vertical bars, was observed in GT and BT, except that the peduncle and tail of the BT is dark black (C) due to further aggravated melanophores. (D–F) Higher magnification of green box in A–C. Many xanthophores (blue box in D) and erythrophores (white box in D) were observed in the tail fin of WT (A, D), while few xanthophores and erythrophores were observed in GT (B, E) and BT (C, F). (G–H) Statistical analysis of the density of melanophores in WT, GT and BT (box area in A–C). The highest density of melanophores was observed on caudal peduncle (CP) (red box) of BT, followed by bar area (blue box) of WT, and then interbar area (white box) of WT, caudal peduncle area (red box) of WT, pseudo bar (PB) area (blue box) of GT, caudal peduncle area (red box) of GT, pseudo bar area (blue box) of BT, and there was no significant difference among the latter five (G). For the tail fin, the highest density of melanophores was observed on BT-TF, followed by WT-TF-B, the GT-TF and then by WT-TF-I (H). The bars in different color (blue, white, red, green) in G and H correspond to the same color boxed areas in A–C, respectively. Blue arrows indicate melanophores in D–F. Data are presented as mean ± SD (n = 6 each). Different letters above the error bar indicate significant differences at $p < 0.05$, as determined by one-way ANOVA followed by Tukey test. dpf, days post fertilization; WT, wild type fish; GT, gray tail mutants; BT, black tail mutants; B, bar; I, interbar; TF, tail fin; PB, pseudo bar; CP, caudal peduncle; scale bar in A–C, 1 cm; scale bar in D–F, 1 mm.

the POTS by PCR using BT and WT genomic DNA as templates for Sanger sequencing. The results showed that no mutation was detected in any POTS, thereby excluding any off-target effect for BT phenotype. Therefore, we believe that BT may be caused by a pre-existing allele, and the *csf1ra* mutation probably revealed cryptic polymorphism at another locus. Crosses between target 1 (exon 3) and target 2 (exon 2) mutants are on the way to determine whether BT is linked to *csf1ra* or not. BT is a unique phenotype has never been observed in WT fishes and never obtained by gene editing before.

5. Conclusions

In this study, we established two mutant lines with different target loci of *csf1ra* gene in Nile tilapia and found that *csf1ra* activity is essential for the development of erythrophores, late developing xanthophores and late metamorphic melanophores. However, the establishment of early embryonic pigment cell precursors and the appearance of melanophores on the body in the late stage are independent of *csf1ra*. In contrast, the formation of vertical bar pattern requires the late metamorphic melanophores and the xanthophores dependent on *csf1ra* signal. The *csf1ra* mutants are important animal models for dissecting xanthophore and erythrophore function. Our study may help deepen the understanding of the formation of fish body color pattern, especially for cichlids with vertical bars. In addition, the mutants might be developed as ornamental fish (BT) or new strains for aquaculture.

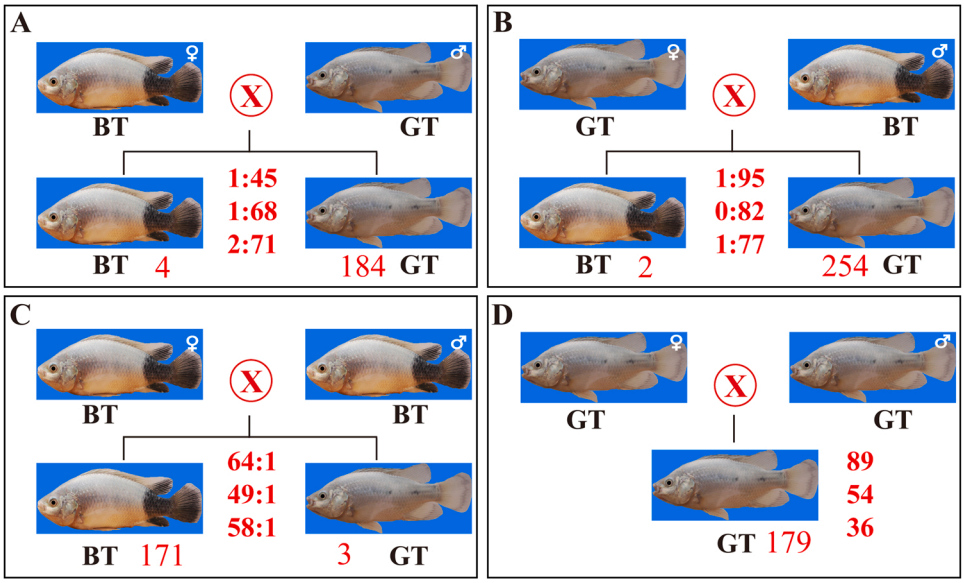

Fig. 7. Crosses and offspring statistics in different GT and BT combinations. Crosses were performed using GT and BT male and female fish in different combinations and repeated three times. The phenotype identification of GT and BT for the offspring was performed at 90 days post fertilization for quantitative statistics. Crosses of BT female and GT male produced BT:GT = 4:184 (1:45, 1:68, 2:71). Crosses of GT female and BT male produced BT:GT = 2:254 (1:95, 0:82, 1:77). Crosses of BT female with BT male produced BT:GT = 171:3 (64:1, 49:1; 58:1). Crosses of GT female and GT male produced BT:GT = 0:179 (89, 54, 36). GT, gray tail mutants; BT, black tail mutants.

CRediT authorship contribution statement

Data curation, **Baoyue Lu** and **Guangyuan Liang**; Investigation, **Baoyue Lu** and **Mengmeng Xu**; Methodology, **Baoyue Lu**; Supervision, **Deshou Wang**; Writing – original draft, **Baoyue Lu**; Writing – review & editing, **Chenxu Wang, Thomas Kocher, Lina Sun** and **Deshou Wang**. All authors read and approved the final manuscript.

Declaration of Competing Interest

The authors declare that they have no known competing financial interests or personal relationships that could have appeared to influence the work reported in this paper.

Acknowledgments

This work was supported by Grants 31872556, 31861123001, 31630082 and 32072963 from the National Natural Science Foundation of China; Grants cstc2021ycjh-bgzxm0024 and CQYC201903173 from the Chongqing Science and Technology Bureau.

Appendix A. Supporting information

Supplementary data associated with this article can be found in the online version at doi:10.1016/j.aqrep.2022.101077.

References

Ahi, E.P., Lecaudey, L.A., Ziegelbecker, A., Steiner, O., Glabonjat, R., Goessler, W., Hois, V., Wagner, C., Lass, A., Sefc, K.M., 2020. Comparative transcriptomics reveals candidate carotenoid color genes in an East African cichlid fish. BMC Genom. 21 (1), 54.

Ban, E., Kasai, A., Sato, M., Yokozeki, A., Hisatomi, O., Oshima, N., 2005. The signaling pathway in photoresponses that may be mediated by visual pigments in erythrophores of Nile tilapia. Pigment Cell Res. 18 (5), 360–369.

Bennett, D.C., Lamoreux, M.L., 2003. The color loci of mice–a genetic century. Pigment Cell Res. 16 (4), 333–344.

Besmer, P., Manova, K., Duttlinger, R., Huang, E.J., Packer, A., Gyssler, C., Bachvarova, R.F., 1993. The *kit*-ligand (steel factor) and its receptor *c-kit/W*: pleiotropic roles in gametogenesis and melanogenesis. Development (Supplement), S125–S137.

Chen, J.L., Fan, Z., Tan, D.J., Jiang, D.N., Wang, D.S., 2018. A review of genetic advances related to sex control and manipulation in tilapia. J. World Aquac. Soc. 49, 277–291.

Chen, S.C., Hornsby, M.A., Robertson, R.M., Hawryshyn, C.W., 2014. The influence of chromatic background on the photosensitivity of tilapia erythrophores. Biol. Open 3 (2), 117–120.

Chen, S.C., Xiao, C., Troje, N.F., Robertson, R.M., Hawryshyn, C.W., 2015. Functional characterisation of the chromatically antagonistic photosensitive mechanism of erythrophores in the tilapia *Oreochromis niloticus*. J. Exp. Biol. 218 (Pt 5), 748–756.

Du, J., Chen, H., Mandal, B.K., Wang, J., Shi, Z., Lu, G., Wang, C., 2021. HDL receptor/scavenger receptor b1 *scarb1* and *scarb1-like* mediate the carotenoid-based red coloration in fish. Aquaculture 545 (2), 737208.

Eriksson, J., Larson, G., Gunnarsson, U., Bed'hom, B., Tixier-Boichard, M., Strömstedt, L., Wright, D., Jungerius, A., Vereijken, A., Randi, E., Jensen, P., Andersson, L., 2008. Identification of the yellow skin gene reveals a hybrid origin of the domestic chicken. PLoS Genet. 4 (2), e1000010.

Fang, J., Chen, T., Pan, Q., Wang, Q., 2018. Generation of albino medaka (*Oryzias latipes*) by CRISPR/Cas9. J. Exp. Zool. Part B. Mol. Dev. Evol. 330, 242–246.

Food and Agriculture Organization (FAO), 2020. The State of World Fisheries and Aquaculture. Rome, Italy. Available from URL: ⟨http://www.fao.org/publications/card/en/c/CA9229EN⟩, (Accessed 6 May 2021).

Fujii, R., 2000. The regulation of motile activity in fish chromatophores. Pigment Cell Res. 13, 300–319.

Fujimura, K., Okada, N., 2007. Development of the embryo, larva and early juvenile of Nile tilapia *Oreochromis niloticus* (Pisces: Cichlidae). Developmental staging system. Dev. Growth Differ. 49 (4), 301–324.

Hendrick, L.A., Carter, G.A., Hilbrands, E.H., Heubel, B.P., Schilling, T.F., Le Pabic, P., 2019. Bar, stripe and spot development in sand-dwelling cichlids from Lake Malawi. EvoDevo 10, 18.

Herbomel, P., Thisse, B., Thisse, C., 2001. Zebrafish early macrophages colonize cephalic mesenchyme and developing brain, retina, and epidermis through a M-CSF receptor-dependent invasive process. Dev. Biol. 238 (2), 274–288.

Hilsdorf, A.W., Penman, D.J., Farias, E.C., McAndrew, B., 2002. Melanophore appearance in wild and red tilapia embryos. Pigment Cell Res. 15 (1), 57–61.

Hirata, M., Nakamura, K., Kanemaru, T., Shibata, Y., Kondo, S., 2003. Pigment cell organization in the hypodermis of zebrafish. Dev. Dyn.: Off. Publ. Am. Assoc. Anat. 227 (4), 497–503.

Johnson, S.L., Africa, D., Walker, C., Weston, J.A., 1995. Genetic control of adult pigment stripe development in zebrafish. Dev. Biol. 167 (1), 27–33.

Kelsh, R.N., Harris, M.L., Colanesi, S., Erickson, C.A., 2009. Stripes and belly-spots – a review of pigment cell morphogenesis in vertebrates. Semin. Cell Dev. Biol. 20 (1), 90–104.

Kottler, V.A., Fadeev, A., Weigel, D., Dreyer, C., 2013. Pigment pattern formation in the guppy, *Poecilia reticulata*, involves the Kita and Csf1ra receptor tyrosine kinases. Genetics 194 (3), 631–646.

Lang, M.R., Patterson, L.B., Gordon, T.N., Johnson, S.L., Parichy, D.M., 2009. Basonuclin-2 requirements for zebrafish adult pigment pattern development and female fertility. PLoS Genet. 5 (11), e1000744.

Lopes, R.J., Johnson, J.D., Toomey, M.B., Ferreira, M.S., Araujo, P.M., Melo-Ferreira, J., Andersson, L., Hill, G.E., Corbo, J.C., Carneiro, M., 2016. Genetic basis for red coloration in birds. Curr. Biol.: CB 26 (11), 1427–1434.

Lu, B., Liang, G., Xu, M., Wang, C., Tan, D., Tao, W., Sun, L., Wang, D., 2022. Production of all male amelanotic red tilapia by combining MAS-GMT and *tyrb* mutation. Aquaculture 546 (Web Server issue), 737327.

Maderspacher, F., Nüsslein-Volhard, C., 2003. Formation of the adult pigment pattern in zebrafish requires leopard and obelix dependent cell interactions. Development 130 (15), 3447–3457.

Mills, M.G., Patterson, L.B., 2009. Not just black and white: pigment pattern development and evolution in vertebrates. Semin. Cell Dev. Biol. 20 (1), 72–81.

Mundy, N.I., Stapley, J., Bennison, C., Tucker, R., Twyman, H., Kim, K.W., Burke, T., Birkhead, T.R., Andersson, S., Slate, J., 2016. Red carotenoid coloration in the zebra

finch is controlled by a cytochrome P450 gene cluster. Curr. Biol.: CB 26 (11), 1435–1440.
Parichy, D.M., 2006. Evolution of danio pigment pattern development. Heredity 97 (3), 200–210.
Parichy, D.M., Mellgren, E.M., Rawls, J.F., Lopes, S.S., Kelsh, R.N., Johnson, S.L., 2000b. Mutational analysis of endothelin receptor b1 (*rose*) during neural crest and pigment pattern development in the zebrafish *Danio rerio*. Dev. Biol. 227 (2), 294–306.
Parichy, D.M., Ransom, D.G., Paw, B., Zon, L.I., Johnson, S.L., 2000a. An orthologue of the kit-related gene *fms* is required for development of neural crest-derived xanthophores and a subpopulation of adult melanocytes in the zebrafish, *Danio rerio*. Development 127 (14), 3031–3044.
Parichy, D.M., Rawls, J.F., Pratt, S.J., Whitfield, T.T., Johnson, S.L., 1999. Zebrafish sparse corresponds to an orthologue of *c-kit* and is required for the morphogenesis of a subpopulation of melanocytes, but is not essential for hematopoiesis or primordial germ cell development. Development 126 (15), 3425–3436.
Parichy, D.M., Turner, J.M., 2003a. Temporal and cellular requirements for Fms signaling during zebrafish adult pigment pattern development. Development 130 (5), 817–833.
Parichy, D.M., Turner, J.M., 2003b. Zebrafish puma mutant decouples pigment pattern and somatic metamorphosis. Dev. Biol. 256 (2), 242–257.
Salzburger, W., Braasch, I., Meyer, A., 2007. Adaptive sequence evolution in a color gene involved in the formation of the characteristic egg-dummies of male *haplochromine* cichlid fishes. BMC Biol. 5, 51.
Sambrook, J., Fritsch, E.F., Maniatis, T., 1989. Molecular Cloning: A Laboratory Manual, 2nd ed. Cold Spring Harbor Laboratory, Cold Spring Harbor, NY.
Sköld, H.N., Aspengren, S., Cheney, K.L., Wallin, M., 2016. Fish chromatophores–from molecular motors to animal behavior. Int. Rev. Cell Mol. Biol. 321, 171–219.
Toews, D.P., Taylor, S.A., Vallender, R., Brelsford, A., Butcher, B.G., Messer, P.W., Lovette, I.J., 2016. Plumage genes and little else distinguish the genomes of hybridizing warblers. Curr. Biol.: CB 26 (17), 2313–2318.
Toomey, M.B., Lopes, R.J., Araújo, P.M., Johnson, J.D., Gazda, M.A., Afonso, S., Mota, P. G., Koch, R.E., Hill, G.E., Corbo, J.C., Carneiro, M., 2017. High-density lipoprotein receptor SCARB1 is required for carotenoid coloration in birds. Proc. Natl. Acad. Sci. USA 114 (20), 5219–5224.
Tripathy, P.S., Devi, N.C., Parhi, J., Priyadarshi, H., Patel, A.B., Pandey, P.K., Mandal, S. C., 2019. Molecular mechanisms of natural carotenoid-based pigmentation of Queen Loach, *Botia dario* (Hamilton, 1822) under captive condition. Sci. Rep. 9 (1), 12585.
Twyman, H., Valenzuela, N., Literman, R., Andersson, S., Mundy, N.I., 2016. Seeing red to being red: conserved genetic mechanism for red cone oil droplets and co-option for red coloration in birds and turtles. Proc. Biol. Sci. 283 (1836), 20161208.
Wang, C., Lu, B., Li, T., Liang, G., Xu, M., Liu, X., Tao, W., Zhou, L., Kocher, T.D., Wang, D., 2021. Nile Tilapia: a model for studying teleost color patterns. J. Hered. 112 (5), 469–484.
Zhu, W., Wang, L., Dong, Z., Chen, X., Song, F., Liu, N., Yang, H., Fu, J., 2016. Comparative transcriptome analysis identifies candidate genes related to skin color differentiation in red tilapia. Sci. Rep. 6, 31347.
Zsebo, K.M., Williams, D.A., Geissler, E.N., Broudy, V.C., Martin, F.H., Atkins, H.L., Hsu, R.Y., Birkett, N.C., Okino, K.H., Murdock, D.C., 1990. Stem cell factor is encoded at the Sl locus of the mouse and is the ligand for the c-kit tyrosine kinase receptor. Cell 63 (1), 213–224.